

Local-Selective Feature Distillation for Single Image Super-Resolution

SeongUk Park, Nojun Kwak
Seoul National University
Seoul, Korea

{swpark0703, nojunk}@snu.ac.kr

Abstract

Recent improvements in convolutional neural network (CNN)-based single image super-resolution (SISR) methods rely heavily on fabricating network architectures, rather than finding a suitable training algorithm other than simply minimizing the regression loss. Adapting knowledge distillation (KD) can open a way for bringing further improvement for SISR, and it is also beneficial in terms of model efficiency. KD is a model compression method that improves the performance of Deep Neural Networks (DNNs) without using additional parameters for testing. It is getting the limelight recently for its competence at providing a better capacity-performance tradeoff. In this paper, we propose a novel feature distillation (FD) method which is suitable for SISR. We show the limitations of the existing FitNet-based FD method that it suffers in the SISR task, and propose to modify the existing FD algorithm to focus on local feature information. In addition, we propose a teacher-student-difference-based soft feature attention method that selectively focuses on specific pixel locations to extract feature information. We call our method local-selective feature distillation (LSFD) and verify that our method outperforms conventional FD methods in SISR problems.

1. Introduction

Single image super-resolution (SISR) [9] is an important task in computer vision and image processing, which aims to generate high-resolution images, I_{SR} , from degraded low-resolution images, I_{LR} , using the ground truth high-resolution images, I_{HR} , as the training dataset. Among the prior works, SRCNN [7] is the first to propose to use convolutional neural networks (CNNs) in SISR problems. It outperformed the other prior works by using only three convolution layers. Afterward, numerous CNN-based super-resolution (SR) methods [44] that contributed to the progress of super-resolution have been proposed so far.

EDSR [28] reported that networks with larger capacity and longer training iterations are directly related to high per-

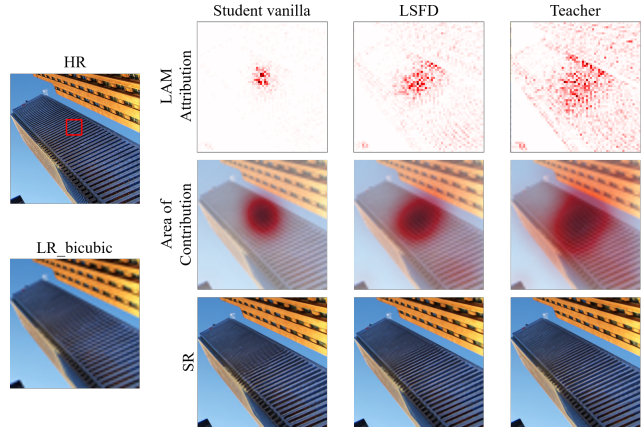


Figure 1. Visualization of local attribution map [11] for the vanilla student network, student network trained using our proposed feature distillation method (LSFD), and teacher network. The student networks are small RCAN [49], and the teacher network is original RCAN, with scale $\times 4$ image.

formance because deeper super-resolution networks attain larger receptive fields, which enable the network to learn the complicated mapping between I_{LR} and I_{HR} . Through residual scaling, EDSR succeeded in stably training the network with deeply stacked residual blocks [14] without using any batch normalization layer, and this brought significant performance improvement. After the success of EDSR, networks with a larger number of parameters or computations were preferred for performance improvement.

However, since the super-resolution techniques are usually used as a preprocessing for a bigger task, it is also very important whether the trained network is practical with concerning the model size and the computational complexity. Especially for resource-limited environments such as mobile chips and embedded systems, lightweight networks are generally preferred. In the field of super-resolution, many studies built lightweight networks to improve model efficiency [5, 8, 22, 49]. The studies are generally divided into four categories: 1) efficient network design, 2) model pruning, 3) quantization, and 4) knowledge distillation.

Among the four methods, we focus on knowledge distillation (KD) [18], especially feature-map level knowledge distillation (FD). Adapting KD for super-resolution is advantageous in two points: 1) Super-resolution generally requires more computations for performance improvements which always have to negotiate with the model efficiency, 2) Introducing additional loss terms that can improve the performance of SISR other than the vanilla L_1 loss term has not been well studied.

KD was firstly proposed for the classification problem, and contemporary studies in the field of KD mainly focus on the task of abstraction, such as classification, object detection, and semantic segmentation. To distill knowledge in the tasks other than the classification, feature-map-level knowledge distillation methods are used broadly in order to deliver rich information learned by a stronger teacher network to a student network. As we will show later in our ablation studies, the conventional distance-based FD method combined with the regressor, which is composed of 1×1 convolution layer with ReLU activation [34], suffers in the task of super-resolution.

As a solution, in this paper, we propose a FD method for a super-resolution model called LSFD, which is an abbreviation of Local-Selective Feature Distillation. Existing methods propose mimicking the information at each feature location through a distance loss or distilling information about the relation between every other pixel location for the student network. On the other hand, our feature distillation method proposes that information at each pixel location in the feature map only affects the distillation of several neighboring pixels, so that the student network can utilize its receptive fields effectively, which is called local feature distillation (LFD). Also, we added an attention function named selective feature distillation (SFD) based on the teacher-student error to further enhance our feature distillation performance. By binding them, we propose a novel feature distillation method designed for SISR, called local-selective feature distillation (LSFD). An example of visualizing our method is in Figure 1, using the method of LAM [11], showing that our method allows the student model to well-utilize its receptive fields. We will discuss more and show more examples in supplementary materials. The main contributions of our paper are:

- We propose local feature distillation (LFD), which is a straightforward method that expands the receptive field of feature distillation locally to alleviate the problems of the conventional distance-based feature distillation methods in super-resolution.
- We also propose selective feature distillation (SFD) that uses an attention mechanism for the feature maps in the knowledge distillation, which grants further improvements to LFD, called local-selective feature distillation

(LSFD).

- We demonstrate the effectiveness of our LSFD on several well-known benchmark models and datasets, and achieve performance improvements at single image super-resolution on most benchmarks having different resolutions.

2. Related Work

2.1. CNN-based Super-resolution

CNN-based models learn the mapping from I_{LR} to I_{HR} directly. After SRCNN [7] which used a simple CNN model for SR, many deep-learning-based algorithms outperformed traditional methods [19, 43, 47] by far, and many CNN-based algorithms [5, 13, 21, 22, 28, 39, 49, 51] contributed to performance improvement in the field of SISR. Though SRCNN expected that stacking more layers would lead to performance improvement, this has not been easily achieved due to the vanishing gradient problem. Later, this problem was solved due to the advent of residual blocks [14]. Using residual blocks, VDSR [21], and DRCN [22] developed networks with deeply stacked residual blocks to improve performance. Furthermore, EDSR [28] largely improved the performance of SISR by eliminating the batch normalization [20], claiming that the batch normalization regularizes the representation power of the model. However, it was difficult to stably train a deep model without batch normalization. For a solution, EDSR suggested using residual scaling, and succeed in stably training a deep and wide network with 32 residual blocks and 256 channels.

Relatively recently, methods adopting various attention mechanisms [1, 42] are thriving in the field of single image super-resolution. RCAN [49] used residual channel attention blocks and showed impressive performance enhancement. Though few years have passed, RCAN still serves as a strong baseline method that frequently takes the second-best place in many state-of-the-art benchmarks [5, 35]. RAM [24] used intra-channel attention as well as inter-channel attention and recorded comparable performance. Algorithms using spatial attention have also been proposed. SAN [5] proposed second-order channel attention (SOCA) and non-locally enhanced residual group (NLRG) to refine features using feature statistics. HAN [35] proposed the layer attention module (LAM) and the channel-spatial attention module (CSAM) that collaboratively consider multi-scale layers, and improved the SISR results. However, spatial attentions or non-local operations come with many shortcomings: they occupy huge memory and slow down the inference speed in GPUs at test time, which limit their usage in practice.

2.2. Efficient Single Image Super-resolution

Given a low-resolution image I_{LR} , a SISR network outputs a super-resolution image I_{SR} that aims to reconstruct the high-resolution image I_{HR} . In the training of a network for SISR, it is common to use cropped patches of the original images as I_{LR} and I_{HR} , and for testing, the network uses the whole original image as I_{LR} . Since the SISR network only learns with the cropped small patches, there is a large discrepancy between the training and testing. A common phenomenon is that the network fails to reconstruct the local patterns at the test phase, even though it can be inferred from the neighboring pixels in a human sense. Thus, many recent works in SISR [5, 29, 33, 35] proposed using non-local operations to enhance the performance. However, non-local operations involve extra operations that often require huge computations at test time since the complexity of a non-local operation may increase at least asymptotically linear [33] or quadratic [5] to the input size, i.e. $O(NC)$ or $O(N^2C^2)$, where $N = H \times W$ when the height of the input image is H , and the width is W , and C is the channel size of the SISR network. Although the non-local operation may not largely increase the parameter of the network, forwarding large test images occupies huge memory and requires lots of time consumption. Thus, networks with good computation-to-performance tradeoffs are preferred in most situations but will be particularly preferred in resource-limited embedded systems, and many lightweight networks are recently proposed [3, 12, 30, 31] that focus on designing a good network for efficient super-resolution.

2.3. Feature-map-level Knowledge Distillation

KD [18] proposed training a student network to learn soft-labels extracted from a larger teacher network, and achieved meaningful improvements. One shortcoming of this label-based approach is that the original KL-divergence-based loss is not applicable to tasks other than image classification, so that feature-map-level distillation would be preferred for researchers who want to apply knowledge distillation to other forms of tasks. In the early studies, AT [45] proposed to distill simple attention map, which is made by simply summing up the channel activations in the channel direction, and achieved comparable results to KD. FitNet [37] proposed using both label information and feature information. For feature information, they proposed to use a regressor, which is made of a 1×1 convolution layer, claiming that it can cope with the channel difference between the teacher network and the student network. This simple transformation using 1×1 convolution became the key element in future feature distillation researches [4, 16, 17, 23, 36]. This regressor is also used in other studies that adapted feature distillation, such as object detection [2, 6, 41, 46].

For super-resolution, Zhang et al. [48] proposed distill-

ing knowledge in super-resolution with training data. Lee et al. [26] enhanced FSRCNN [8] using an autoencoder [32] that is trained by reconstructing the I_{HR} , and trained the FSRCNN to mimic the intermediate feature of the autoencoder. The most related study to our work is FAKD [15], which proposed distilling the feature-affinity matrix of the teacher network to the student network, which improved the performance of SAN and RCAN.

3. Proposed Method

In this work, we focus on a promising solution that has not been spotlighted much in SISR: knowledge distillation which makes the trained network more efficient, and operates in the level of the loss function. To the best of our knowledge, only a few studies [15, 26] exist that adopt knowledge distillation for super-resolution.

3.1. Knowledge distillation for SISR

Adapting knowledge distillation in the field of single image super-resolution is promising in two aspects. **First**, whereas finding an efficient network architecture for SISR has been extensively studied, researches that seek for finding improved training methodologies other than a simple L_1 regression loss are lacking. Since knowledge distillation generally grants performance improvements with additional loss terms to the conventional loss term, adopting knowledge distillation can bring further improvements in the field of single image super-resolution. **Second**, using knowledge distillation for SISR is meaningful for the model in the view of efficiency. As explained in Section 2.1, recent developments in SISR mostly depend on non-local operations for their performance improvements [5, 24, 29, 33, 35]. Although non-local operations are parameter-efficient because non-local operations do not use additional parameters, they occupy huge GPU memory at test time, which will be shown in Section 4.1.

To adapt knowledge distillation, a straightforward approach is using the output super-resolution image of the teacher I_{SR}^T as the learning target. Thus the loss function for the student I_{SR}^S is:

$$\mathcal{L}_{SR} = \frac{1}{2N} \left(\sum_{n=1}^N \|I_{SRn}^T - I_{SRn}^S\|_1 + \sum_{n=1}^N \|I_{HRn} - I_{SRn}^S\|_1 \right), \quad (1)$$

where N refers to the number of training samples in a mini-batch. It is also worth considering using rich feature information, called feature distillation. One plausible and straightforward option to consider when adapting feature distillation is to use the regressor [37] which was mentioned in Section 2.3, because it has shown its effectiveness on the tasks other than image classification [2, 6, 41, 46]. However, it has shown to be ineffective in the experiment in FAKD [15]. We also report this problem later in our experiment.

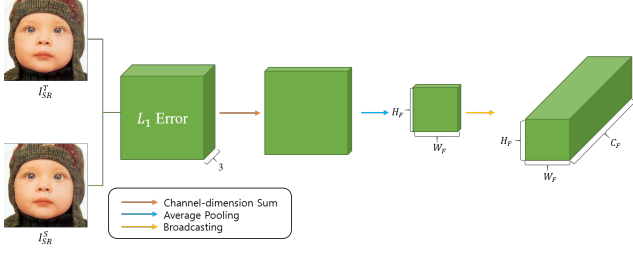


Figure 3. Detailed illustration of SFD. H_F , W_F , and C_F refers to the height, width, and the channel size of the distilled feature maps at the intermediate layers.

in the surrounding pattern, especially when there exists a specific pattern that repeats within an image.

3.3. Selective Feature Distillation

To further improve LFD, we propose *selective feature distillation* (SFD) which calculates an attention map for the feature distillation location. Merging LFD and SFD together, we call our method *local-selective feature distillation* (LSFD). Because FD adds an auxiliary loss to the conventional \mathcal{L}_{SR} loss, it is natural for FD to attend more to the feature map positions where the student and the teacher disagree much and let the \mathcal{L}_{SR} loss take care of the other positions. This motivates us to pay more attention to the positions where the difference between I_{SR}^T and I_{SR}^S is large. For SFD, the detailed process for obtaining the attention map is depicted in Figure 3, and it is formulated as:

$$SFD = B(P(\sum_{n=1}^3 \|I_{SRn}^T - I_{SRn}^S\|_1, S), C), \quad (3)$$

where $P(\cdot, S)$ is spatial average pooling over the tensor with a kernel size of S , and S refers to the scale ratio of the model training, and $B(\cdot, C)$ represents the broadcasting operation over the channel dimension with C being the channel size of the feature map in the SISR network. Since SISR networks do not increase the spatial dimension of the intermediate features and only adapt the pixelshuffle operation at the end of the network, the pooled and broadcasted tensor has the same size as the intermediate feature maps.

This is a big difference compared to FAKD [15], which proposed to learn the feature correlation of different feature map positions by distilling a correlation matrix with $HW \times HW$ size. In FAKD, calculating correlation matrix is a non-local operation, so that the student network is forced to learn feature relations from every feature position pair, even though there may exist unnecessary pairs that are less related, i.e. features on different positions that are distant, or features that are not lying on the same object. We thought that it would be more helpful to focus on the more informative pixels. To this end, we use SFD as an attention operator to LFD presented in Sec. 3.2.

Model Configuration	RCAN		EDSR		SAN	
	T	S	T	S	T	S
Channel Size	64	64	256	64	64	64
Resblocks	20	6	32	16	10	10
ResGroups	10	10	-	-	20	6
Params (M)	15.59	5.17	43	1.5	15.86	5.0
Runtime (ms)	117	42	171	14	2670	806
GPU Memory (GiB)	1.29	1.20	1.83	1.18	17.75	17.71
MultiAdds (T)	4.70	1.53	12.51	0.42	-	-

Table 1. Model configurations and their efficiency indicators for the RCAN, EDSR, and SAN networks that were experimented in this paper.

The final LSFD loss is derived by element-wise multiplication of SFD and D matrix. Combining all the loss terms together, the final total loss is:

$$\mathcal{L}_{LSFD} = \alpha_2 \|SFD \otimes D\|_1 \quad (4)$$

$$\mathcal{L}_{total} = \mathcal{L}_{LSFD} + \mathcal{L}_{SR} \quad (5)$$

where \otimes denotes to the element-wise multiplication, and α_2 is a hyper-parameter for scaling the \mathcal{L}_{LSFD} to match the loss scale of \mathcal{L}_{SR} .

4. Experiments

In this section, we first explain the details of our network training, and analyze the experimental results both quantitatively and qualitatively.

4.1. Experiment Settings

Following the previous literature [5, 7, 21, 28, 49], we use 800 images from DIV2K [40] dataset for the network training, and use Set5, Set14, BSD100 and Urban100 dataset for testing the trained network, each having different characteristics. We conducted experiments on three SISR networks, RCAN [49], EDSR [28], and SAN [5]. All the student networks are trained using ADAM [25] optimizer with $\beta_1 = 0.9$, $\beta_2 = 0.99$, and $\epsilon = 10^{-8}$. The initial learning rate is 0.0001, and is halved at 150 epochs. The main comparator in our experiments was FAKD [15]. FAKD trained the student network for 200 epochs, but empirically, this was far from the point of saturation. Therefore, we trained all the student networks for 300 epochs. All the networks use mini-batches containing 16 low-resolution patches whose size is 48×48 for input, and only horizontal flip was applied for data augmentation. Random rotation was not applied to exclude possible interactions with feature distillation, which is different from the training of the original SAN. For LFD, α_1 is set to 2,000, and α_2 is set to 10 in Eq. (2) and Eq. (4).

For the network architecture, the teacher network of the RCAN has 20 residual channel attention blocks (RCAB) in every 10 residual groups (RG) and 64 feature map channels. For the student network of RCAN, the number of RCABs

in each RG is changed to 6; thus, the student network has about 1/3 parameters compared to the teacher network. In contrast, for SAN, we maintain the residual blocks in each local-source residual attention group (LSRAGs) as 10 but reduce the number of LSRAGs from 20 for the teacher network to 6 for the student network. For both types of networks, we maintain the number of channels for the student networks. For EDSR, we reduce the number of residual blocks and the number of channels from 32 and 256 to 16 and 64.

Some measures for the models which we experimented with are provided in Table 1, together with the model configurations explained above. The ‘Memory’ refers to the amount of GPU memory consumption at the test phase, and the runtime is the average time taken for processing an input image. The runtime and memory usage are measured using 100 images in the B100 benchmark dataset with the upscale ratio of 2 and batch size of 1, using a single Geforce Titan RTX GPU. The MultiAdds is calculated using single $3 \times 640 \times 480$ sized input, and the GPU memory consumption in the table is the ceiling value required to measure the entire data set. Since EDSR only has resblocks, numbers on the ResGroups row are omitted. For SAN, the SOCA block of SAN has intractable calculations because it handles heavy operations, which includes $HWC \times HWC$ sized covariance matrix, so the MultiAdds row is omitted.

4.2. Quantitative Results

The quantitative results are in Table 2, 3, 4. In this subsection, we analyze the results on these tables based on several different criteria.

Impact of deeper regressor: From Table 2, we can compare the result of FitNet and LFD. When FitNet is used directly on SISR, a slight increase in the PSNR scores occurs. By making the regressor much deeper, each pixel learns from more spacious features from the teacher network so that the student network learns to focus on local regions that may help reconstruct local patterns. Thus, LFD is much more suitable for SISR, leading to the success of feature distillation in super-resolution.

Impact of LFD and LSFD: In Table 2 and 3, the test PSNR estimated using our LSFD outperforms the previous methods in most of the experiments. Our LFD and LSFD especially perform better in Urban100 dataset, where reconstructing repetitive local patterns is essential, as we intended. However, this effect diminishes in a high scale ratio ($\times 4$). We conjecture that the information loss is so significant that the local patterns are no longer helpful in reconstructing the original. For all training methods, the increases in PSNR in EDSR are poorer on average compared to RCAN, but LSFD performed better than others in most settings. We conjecture that the reason for the inferior feature distillation performances in EDSR is using a long skip

RCAN					
Scale	Methods	Set5	Set14	B100	Urban100
$\times 2$	Teacher	38.271	34.126	32.390	33.176
	Student	38.074	33.623	32.199	32.317
	FAKD	38.164	33.815	32.274	32.533
	FAKD*	38.180	33.828	32.284	32.602
	FitNet	38.132	33.759	32.253	32.460
	LFD	38.178	33.840	32.296	32.669
	LSFD	38.189	33.882	32.291	32.704
	FAKD + FFT	38.187	33.866	32.289	32.669
$\times 3$	Teacher	34.758	30.627	29.309	29.104
	Student	34.557	30.408	29.162	28.482
	FAKD	34.653	30.449	29.208	28.523
	FAKD*	34.667	30.490	29.209	28.611
	FitNet	34.570	30.466	29.184	28.493
	LFD	34.657	30.525	29.224	28.665
	LSFD	34.666	30.510	29.226	28.689
	FAKD + FFT	34.666	30.527	29.218	28.635
$\times 4$	Teacher	32.638	28.851	27.748	26.748
	Student	32.321	28.688	27.634	26.340
	FAKD	32.462	28.750	27.678	26.422
	FAKD*	32.461	28.779	27.685	26.490
	FitNet	32.417	28.716	27.660	26.406
	LFD	32.475	28.783	27.693	26.542
	LSFD	32.497	28.771	27.699	26.525
	FAKD + FFT	32.491	28.755	27.693	26.507
$\times 4$	LSFD + FFT	32.513	28.774	27.709	26.535

Table 2. PSNR scores measured on RCAN networks. The scores on the FAKD row are from its original paper, and the scores on FAKD* row are our reproduced scores with longer training epochs. The red and blue text is the best and second-best scores in different combinations of datasets and scales. For the models trained using FFT loss, the scores that outperformed the best scores among the other models without FFT were highlighted in bold fonts.

connection instead of several short skip connections. The LFD seems to be inferior compared to FAKD in EDSR models, but by introducing SFD, LSFD overtakes FAKD.

Adding Frequency-domain loss: We also tried using the frequency domain loss and reported the results in Table 2 and 3. There were a few papers that proposed using frequency domain information. Li et al. [27] proposed using frequency domain inputs for super-resolution, and some other papers [10, 38] suggested frequency component of the I_{SR} for perceptual loss in perceptual super-resolution. In our experiments, we simply use Fourier transformation for our loss:

$$\mathcal{L}_{FFT} = \|\text{FFT}(I_{SR}^S) - \text{FFT}(I_{SR}^T)\|_1, \quad (6)$$

where $\text{FFT}(\cdot)$ is fast Fourier transformation. Using \mathcal{L}_{FFT} was not much help for the RCAN models but was effective for EDSR models. The usage of \mathcal{L}_{FFT} had desirable synergy with both LSFD and FAKD.

EDSR					
Scale	Methods	Set5	Set14	B100	Urban100
$\times 2$	Teacher	38.090	33.797	32.241	32.373
	Student	37.919	33.478	32.126	31.840
	FAKD*	37.976	33.523	32.156	31.906
	LFD	37.984	33.547	32.156	31.896
	LSFD	37.991	33.529	32.157	31.936
	FAKD + FFT	38.004	23.547	32.156	31.928
$\times 3$	Teacher	34.547	30.435	29.167	28.470
	Student	34.272	30.266	29.044	27.959
	FAKD*	34.356	30.296	29.066	28.016
	LFD	34.348	30.287	29.068	27.999
	LSFD	34.384	30.302	29.077	28.029
	FAKD + FFT	34.356	30.312	29.078	28.057
$\times 4$	Teacher	32.385	28.741	27.661	26.425
	Student	32.102	28.526	27.538	25.905
	FAKD*	32.138	28.547	27.557	25.972
	LFD	32.107	28.524	27.552	25.962
	LSFD	32.107	28.548	27.563	25.980
	FAKD + FFT	32.174	28.556	27.562	26.008
	LSFD + FFT	32.140	28.561	27.570	26.003

Table 3. PSNR scores measured on EDSR networks. The meaning of the asterisk, blue, red, bold texts are the same as Table 2.

SAN					
Scale	Methods	Set5	Set14	B100	Urban100
$\times 2$	Teacher	38.144†	33.806†	32.378	32.673†
	Student	38.039†	33.700†	32.211	32.358†
	FAKD*	38.107†	33.738†	32.267	32.558†
	LSFD	38.131†	33.781†	33.276	32.562†
$\times 3$	Teacher	34.642	30.492	29.206	29.166†
	Student	34.461	30.397	29.129	28.394†
	FAKD*	34.638	30.464	29.194	28.540†
	LSFD	34.627	30.468	29.197	28.594†
$\times 4$	Teacher	32.398	28.754	27.696	26.557†
	Student	32.298	28.683	27.622	26.329†
	FAKD*	32.380	28.746	27.679	26.466†
	LSFD	32.413	28.733	27.681	26.453†

Table 4. PSNR scores measured on SAN networks. The numbers with † means it was tested in four-crops, and the FAKD* is our reproduced result.

Results on SAN: For the results in Table 4, there exist limits for a fair comparison because some results contain 4-crop testing, which means we divide each test image in quarter size to generate four of small I_{SR} s, and attached them together later. This drops PSNR because the network cannot get full advantage of non-local operation. However, it was inevitable in order to measure the PSNR because SAN networks require a huge number of operations with $O(N^2C^2)$ complexity, and test images often have a high spatial dimension. For the numbers with * marks, PSNR was measured



Urban100 (2x): Img012.png

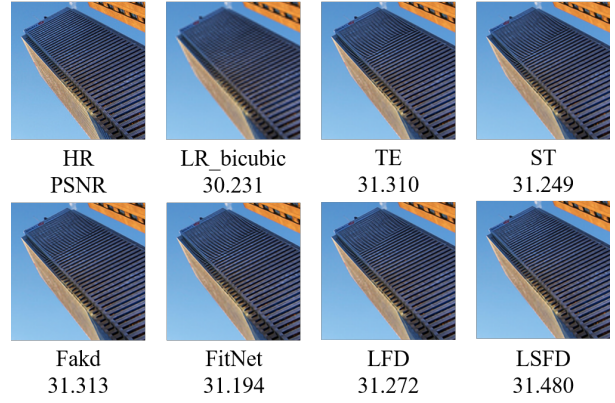
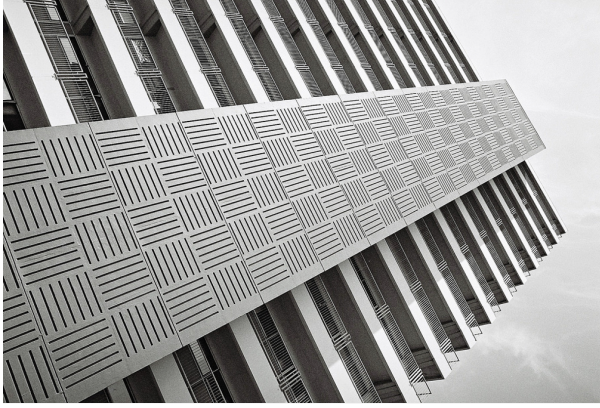


Figure 4. Visual comparison of different training methods on re-constructed images ($\times 2$).

by dividing I_{LR} into quadrants and stitching four small SRs since it was impossible to forward full I_{LR} image using a minibatch of size 1 with RTX A6000 GPU which has 48GB memory.

4.3. Qualitative Results

Detailed visualizations of the difficult Urban100 examples for different RCAN networks are provided in Figure 4, 5 and 6, with each different images and upscale ratios. The images chosen are frequently used samples in other SISR papers. The ‘LR_bicubic’ image is attained by simply applying bicubic upsampling to the I_{LR} . To compare the reconstruction power of the model with the PSNR scores directly, PSNR scores are calculated only using the cropped region for detailed comparison. As can be seen in the low-resolution images, the aliasing problem arises that distorts the original patterns, which mainly causes the performance degradation. For such images, the performance of the network is determined by how well it recovers the pattern of the HR using information from the surrounding patterns [11]. We can clearly see that distilled models produce better results. Especially, for Fig. 4, LSFD reconstructs better than



Urban100 (3x): Img092.png

HR	LR bicubic	Teacher	Student
PSNR	28.168	28.909	28.617
Fakd	FitNet	LFD	LSFD
28.671	28.607	28.715	28.786

Figure 5. Visual comparison of different training methods on reconstructed images ($\times 3$).

the teacher network, which is consistent with the quantitative PSNR results that models trained by our method especially perform well on the Urban100 dataset.

5. Discussion

Effective usage of receptive fields: Various feature distillation methods exist that can be adapted to SISR, but many of them are shown to be ineffective in the paper of FAKD [15]. Since our method enables more expansive feature map areas to be involved for each distilled feature position, the student network is forced to focus on several surrounding positions in the feature map, which results in the effective usage of receptive fields, and this effect is visualized through the gradient map of the LAM. In Figure 1, we can infer that in the ‘Area of Contribution’ of LSFD, our LSFD model tries to use **successfully generated area of itself as a reference** for generating the interested area.

Limitations: Although our model improves the performance of the student network a lot, its limitation is that features at different spatial locations that are far away cannot affect each other, even though they may have relations. For this property, although LSFD notably outperforms on anti-aliasing, as we verified on Urban100 experiments, they perform not as well on other datasets. We think that it would be beneficial if the model could simultaneously attend to the more important feature map areas and simultaneously distill features based on the non-local operation. We tried



Urban100 (4x): Img076.png

HR	LR bicubic	Teacher	Student
PSNR	29.262	30.602	30.155
Fakd	FitNet	LFD	LSFD
30.047	30.324	30.595	30.451

Figure 6. Visual comparison of different training methods on reconstructed images ($\times 4$).

some experiments that use attention to the input feature map of FAKD using the SFD matrix, but it led to performance degradation.

6. Conclusion

This paper described the importance of adapting KD to single image super-resolution (SISR) and proposed Local-Selective Feature Distillation (LSFD) that successfully applies the regressor-based feature distillation on the area of SISR. Our LFD showed the importance of utilizing a wider feature range in the receptive field point of view, and by additionally applying SFD, LSFD demonstrates the impact of our selective attention to more important feature areas both quantitatively and qualitatively. Our method suggests a promising viewpoint for future works adapting feature distillation to the task of super-resolution.

References

- [1] Dzmitry Bahdanau, Kyunghyun Cho, and Yoshua Bengio. Neural machine translation by jointly learning to align and translate. *arXiv preprint arXiv:1409.0473*, 2014. 2
- [2] Guobin Chen, Wongun Choi, Xiang Yu, Tony Han, and Manmohan Chandraker. Learning efficient object detection models with knowledge distillation. *Advances in neural information processing systems*, 30, 2017. 3, 4
- [3] Haoyu Chen, Jinjin Gu, and Zhi Zhang. Attention in attention network for image super-resolution. *arXiv preprint arXiv:2104.09497*, 2021. 3
- [4] Inseop Chung, SeongUk Park, Jangho Kim, and Nojun Kwak. Feature-map-level online adversarial knowledge distillation. In *International Conference on Machine Learning*, pages 2006–2015. PMLR, 2020. 3, 4
- [5] Tao Dai, Jianrui Cai, Yongbing Zhang, Shu-Tao Xia, and Lei Zhang. Second-order attention network for single image super-resolution. In *Proceedings of the IEEE/CVF Conference on Computer Vision and Pattern Recognition*, pages 11065–11074, 2019. 1, 2, 3, 5
- [6] Xing Dai, Zeren Jiang, Zhao Wu, Yiping Bao, Zhicheng Wang, Si Liu, and Erjin Zhou. General instance distillation for object detection. In *Proceedings of the IEEE/CVF Conference on Computer Vision and Pattern Recognition (CVPR)*, pages 7842–7851, June 2021. 3, 4
- [7] Chao Dong, Chen Change Loy, Kaiming He, and Xiaoou Tang. Image super-resolution using deep convolutional networks. *IEEE transactions on pattern analysis and machine intelligence*, 38(2):295–307, 2015. 1, 2, 5
- [8] Chao Dong, Chen Change Loy, and Xiaoou Tang. Accelerating the super-resolution convolutional neural network. In *European conference on computer vision*, pages 391–407. Springer, 2016. 1, 3
- [9] William T Freeman, Egon C Pasztor, and Owen T Carmichael. Learning low-level vision. *International journal of computer vision*, 40(1):25–47, 2000. 1
- [10] Dario Fuoli, Luc Van Gool, and Radu Timofte. Fourier space losses for efficient perceptual image super-resolution. *arXiv preprint arXiv:2106.00783*, 2021. 6
- [11] Jinjin Gu and Chao Dong. Interpreting super-resolution networks with local attribution maps. In *Proceedings of the IEEE/CVF Conference on Computer Vision and Pattern Recognition (CVPR)*, pages 9199–9208, June 2021. 1, 2, 4, 7
- [12] Yong Guo, Yongsheng Luo, Zhenhao He, Jin Huang, and Jian Chen. Hierarchical neural architecture search for single image super-resolution. *IEEE Signal Processing Letters*, 27:1255–1259, 2020. 3
- [13] Muhammad Haris, Gregory Shakhnarovich, and Norimichi Ukita. Deep back-projection networks for super-resolution. In *Proceedings of the IEEE conference on computer vision and pattern recognition*, pages 1664–1673, 2018. 2
- [14] Kaiming He, Xiangyu Zhang, Shaoqing Ren, and Jian Sun. Deep residual learning for image recognition. In *Proceedings of the IEEE conference on computer vision and pattern recognition*, pages 770–778, 2016. 1, 2
- [15] Zibin He, Tao Dai, Jian Lu, Yong Jiang, and Shu-Tao Xia. Fakd: Feature-affinity based knowledge distillation for efficient image super-resolution. In *2020 IEEE International Conference on Image Processing (ICIP)*, pages 518–522. IEEE, 2020. 3, 5, 8
- [16] Byeongho Heo, Jeesoo Kim, Sangdoo Yun, Hyojin Park, Nojun Kwak, and Jin Young Choi. A comprehensive overhaul of feature distillation. In *Proceedings of the IEEE/CVF International Conference on Computer Vision*, pages 1921–1930, 2019. 3, 4
- [17] Byeongho Heo, Minsik Lee, Sangdoo Yun, and Jin Young Choi. Knowledge transfer via distillation of activation boundaries formed by hidden neurons. In *Proceedings of the AAAI Conference on Artificial Intelligence*, volume 33, pages 3779–3787, 2019. 3, 4
- [18] Geoffrey Hinton, Oriol Vinyals, and Jeff Dean. Distilling the knowledge in a neural network. *arXiv preprint arXiv:1503.02531*, 2015. 2, 3
- [19] Jia-Bin Huang, Abhishek Singh, and Narendra Ahuja. Single image super-resolution from transformed self-exemplars. In *Proceedings of the IEEE conference on computer vision and pattern recognition*, pages 5197–5206, 2015. 2
- [20] Sergey Ioffe and Christian Szegedy. Batch normalization: Accelerating deep network training by reducing internal covariate shift. In *International conference on machine learning*, pages 448–456. PMLR, 2015. 2
- [21] Jiwon Kim, Jung Kwon Lee, and Kyoung Mu Lee. Accurate image super-resolution using very deep convolutional networks. In *Proceedings of the IEEE conference on computer vision and pattern recognition*, pages 1646–1654, 2016. 2, 5
- [22] Jiwon Kim, Jung Kwon Lee, and Kyoung Mu Lee. Deeply-recursive convolutional network for image super-resolution. In *Proceedings of the IEEE conference on computer vision and pattern recognition*, pages 1637–1645, 2016. 1, 2
- [23] Jangho Kim, SeongUk Park, and Nojun Kwak. Paraphrasing complex network: Network compression via factor transfer. *arXiv preprint arXiv:1802.04977*, 2018. 3, 4
- [24] Jun-Hyuk Kim, Jun-Ho Choi, Manri Cheon, and Jong-Seok Lee. Ram: Residual attention module for single image super-resolution. *arXiv preprint arXiv:1811.12043*, 2:1, 2018. 2, 3
- [25] Diederik P Kingma and Jimmy Ba. Adam: A method for stochastic optimization. *arXiv preprint arXiv:1412.6980*, 2014. 5
- [26] Wonkyung Lee, Junghyup Lee, Dohyung Kim, and Bumsub Ham. Learning with privileged information for efficient image super-resolution. In *European Conference on Computer Vision*, pages 465–482. Springer, 2020. 3
- [27] Junxuan Li, Shaodi You, and Antonio Robles-Kelly. A frequency domain neural network for fast image super-resolution. In *2018 International Joint Conference on Neural Networks (IJCNN)*, pages 1–8. IEEE, 2018. 6
- [28] Bee Lim, Sanghyun Son, Heewon Kim, Seungjun Nah, and Kyoung Mu Lee. Enhanced deep residual networks for single image super-resolution. In *Proceedings of the IEEE Conference on Computer Vision and Pattern Recognition (CVPR) Workshops*, July 2017. 1, 2, 5

- [29] Ding Liu, Bihan Wen, Yuchen Fan, Chen Change Loy, and Thomas S Huang. Non-local recurrent network for image restoration. *arXiv preprint arXiv:1806.02919*, 2018. 3
- [30] Xin Liu, Yuang Li, Josh Fromm, Yuntao Wang, Ziheng Jiang, Alex Mariakakis, and Shwetak Patel. Splitsr: An end-to-end approach to super-resolution on mobile devices. *Proceedings of the ACM on Interactive, Mobile, Wearable and Ubiquitous Technologies*, 5(1):1–20, 2021. 3
- [31] Xiaotong Luo, Yuan Xie, Yulun Zhang, Yanyun Qu, Cuihua Li, and Yun Fu. Latticenet: Towards lightweight image super-resolution with lattice block. In *Computer Vision–ECCV 2020: 16th European Conference, Glasgow, UK, August 23–28, 2020, Proceedings, Part XXII 16*, pages 272–289. Springer, 2020. 3
- [32] Jonathan Masci, Ueli Meier, Dan Cireşan, and Jürgen Schmidhuber. Stacked convolutional auto-encoders for hierarchical feature extraction. In *International conference on artificial neural networks*, pages 52–59. Springer, 2011. 3
- [33] Yiqun Mei, Yuchen Fan, and Yuqian Zhou. Image super-resolution with non-local sparse attention. In *Proceedings of the IEEE/CVF Conference on Computer Vision and Pattern Recognition (CVPR)*, pages 3517–3526, June 2021. 3
- [34] Vinod Nair and Geoffrey E Hinton. Rectified linear units improve restricted boltzmann machines. In *Icml*, 2010. 2
- [35] Ben Niu, Weilei Wen, Wenqi Ren, Xiangde Zhang, Lianping Yang, Shuzhen Wang, Kaihao Zhang, Xiaochun Cao, and Haifeng Shen. Single image super-resolution via a holistic attention network. In *European Conference on Computer Vision*, pages 191–207. Springer, 2020. 2, 3
- [36] SeongUk Park and Nojun Kwak. Feature-level ensemble knowledge distillation for aggregating knowledge from multiple networks. In *ECAI 2020*, pages 1411–1418. IOS Press, 2020. 3, 4
- [37] Adriana Romero, Nicolas Ballas, Samira Ebrahimi Kahou, Antoine Chassang, Carlo Gatta, and Yoshua Bengio. Fitnets: Hints for thin deep nets. *arXiv preprint arXiv:1412.6550*, 2014. 3, 4
- [38] Shane D Sims. Frequency domain-based perceptual loss for super resolution. In *2020 IEEE 30th International Workshop on Machine Learning for Signal Processing (MLSP)*, pages 1–6. IEEE, 2020. 6
- [39] Ying Tai, Jian Yang, Xiaoming Liu, and Chunyan Xu. Memnet: A persistent memory network for image restoration. In *Proceedings of the IEEE international conference on computer vision*, pages 4539–4547, 2017. 2
- [40] Radu Timofte, Eirikur Agustsson, Luc Van Gool, Ming-Hsuan Yang, and Lei Zhang. Ntire 2017 challenge on single image super-resolution: Methods and results. In *Proceedings of the IEEE conference on computer vision and pattern recognition workshops*, pages 114–125, 2017. 5
- [41] Tao Wang, Li Yuan, Xiaopeng Zhang, and Jiashi Feng. Distilling object detectors with fine-grained feature imitation. In *Proceedings of the IEEE/CVF Conference on Computer Vision and Pattern Recognition (CVPR)*, June 2019. 3, 4
- [42] Kelvin Xu, Jimmy Ba, Ryan Kiros, Kyunghyun Cho, Aaron Courville, Ruslan Salakhudinov, Rich Zemel, and Yoshua Bengio. Show, attend and tell: Neural image caption generation with visual attention. In *International conference on machine learning*, pages 2048–2057. PMLR, 2015. 2
- [43] Jianchao Yang, John Wright, Thomas Huang, and Yi Ma. Image super-resolution as sparse representation of raw image patches. In *2008 IEEE conference on computer vision and pattern recognition*, pages 1–8. IEEE, 2008. 2
- [44] Wenming Yang, Xuechen Zhang, Yapeng Tian, Wei Wang, Jing-Hao Xue, and Qingmin Liao. Deep learning for single image super-resolution: A brief review. *IEEE Transactions on Multimedia*, 21(12):3106–3121, 2019. 1
- [45] Sergey Zagoruyko and Nikos Komodakis. Paying more attention to attention: Improving the performance of convolutional neural networks via attention transfer. *arXiv preprint arXiv:1612.03928*, 2016. 3, 4
- [46] Linfeng Zhang and Kaisheng Ma. Improve object detection with feature-based knowledge distillation: Towards accurate and efficient detectors. In *International Conference on Learning Representations*, 2021. 3, 4
- [47] Lei Zhang and Xiaolin Wu. An edge-guided image interpolation algorithm via directional filtering and data fusion. *IEEE transactions on Image Processing*, 15(8):2226–2238, 2006. 2
- [48] Yiman Zhang, Hanting Chen, Xinghao Chen, Yiping Deng, Chunjing Xu, and Yunhe Wang. Data-free knowledge distillation for image super-resolution. In *Proceedings of the IEEE/CVF Conference on Computer Vision and Pattern Recognition*, pages 7852–7861, 2021. 3
- [49] Yulun Zhang, Kunpeng Li, Kai Li, Lichen Wang, Bineng Zhong, and Yun Fu. Image super-resolution using very deep residual channel attention networks. In *Proceedings of the European Conference on Computer Vision (ECCV)*, September 2018. 1, 2, 5
- [50] Yulun Zhang, Kunpeng Li, Kai Li, Bineng Zhong, and Yun Fu. Residual non-local attention networks for image restoration. *arXiv preprint arXiv:1903.10082*, 2019. 4
- [51] Yulun Zhang, Yapeng Tian, Yu Kong, Bineng Zhong, and Yun Fu. Residual dense network for image super-resolution. In *Proceedings of the IEEE conference on computer vision and pattern recognition*, pages 2472–2481, 2018. 2